AIAA JOURNAL
Vol. 30, No. 7, July 1992

# Bending of Tapered Anisotropic Sandwich Plates with Arbitrary Edge Conditions

J. S. Jeon* and C. S. Hong†
*Korea Advanced Institute of Science and Technology, Yusung-Ku, Taejon, Korea 305-701*

**The bending of tapered sandwich plates is analyzed by a new formulation. The tapered sandwich plate consists of an orthotropic core with linear thickness variation and two anisotropic laminated faces with constant thickness. The faces are analyzed by the classical lamination theory. The analysis shows the geometric coupling between the core shear strain and the face normal deflection in the explicit expression existing only for the tapered geometry. The total potential energy is obtained and the Rayleigh-Ritz method is employed for an approximate solution. Present formulation can be applied to arbitrary edge conditions. The structural deflections are calculated for various edge conditions, taper ratios, core moduli ratios, and stacking sequences. The numerical results show that, as the taper ratio increases, the deflection increases up to certain taper ratio and then decreases by the contribution ratio change of each component.**

## Nomenclature

$a, b, c$ = lengths in $x$, $y$, and $s$ directions, respectively
$[A_{ij}]$, $[B_{ij}]$, $[D_{ij}]$ = extensional, coupling, and bending stiffness of face, respectively
$AR$ = aspect ratio, $a/b$
$C^1_{mn} - C^5_{mn}$ = unknown coefficients
$CR$ = core shear moduli ratio, $G_{13}/G^*_{13} = G_{23}/G^*_{23}$
$E_1, E_2, G_{12}, \nu_{12}$ = material properties of faces
$G^*_{13}, G^*_{23}$ = reference transverse shear moduli of core
$G_{13}, G_{23}$ = varied transverse shear moduli of core
$HR$ = taper ratio, $T_0/T_a$
$h_0, h(x)$ = half thicknesses of core at $x = 0$ and at location $x$, respectively
$m, n$ = series terms in $s$ and $y$ directions, respectively
$Q_0(x_0, y_0)$ = vertical concentrated load at upper face
$q_1(s, y)$ = normal distributed load at upper face
$q_2(x, y)$ = vertical distributed load at upper face
$R_x$ = shear rigidity parameter in Ref. 6, $E_1 t_u T_0/2G_{13}b^2(1 - \nu^2_{12})$
$s, y, n$ = local coordinates of each face
$T_0, T_a$ = structural thicknesses at $x = 0$, and $x = a$, respectively
$t_u, t_l$ = thicknesses of upper and lower faces, respectively
$U_{fu}, U_{fl}, U_c$ = strain energies in upper face, lower face, and core, respectively
$u^o, v^o, w^o$ = structural displacements in $x$, $y$, and $z$ directions, respectively
$u_s, u_y, u_n$ = face displacements in $s$, $y$, and $n$ directions, respectively
$V$ = potential energy by external works
$\overline{w}$ = normalized structural deflection, $4w^0 E_1 t_u T_0^2/q_1 a^4(1 - \nu^2_{12})$
$w^*$ = normalized structural deflection in Ref. 6, $w^0 E_1 t_u T_0^2/2q_2 b^4(1 - \nu^2_{12})$
$x, y, z$ = global coordinates of structure
$\beta$ = face slope angle about structural midplane
$\gamma^o_{xz}, \gamma^o_{yz}$ = transverse shear strains in core
$\{\varepsilon^o\}$ = face inplane strain, $[\varepsilon^o_{ss}, \varepsilon^o_{yy}, \gamma^o_{sy}]^T$
$\theta$ = fiber orientation of face layer
$\{\kappa\}$ = face curvature, $[\kappa_{ss}, \kappa_{yy}, \kappa_{sy}]^T$
$\Pi$ = total potential energy, $U_{fu} + U_{fl} + U_c + V$
$\phi_c$ = core rotation angle about reference axes
$\phi^1_{mn} - \phi^3_{mn}$ = shape functions satisfying the given edge conditions

*Subscripts*

$c, f$ = values for core and faces, respectively
$u, l$ = values for upper and lower faces, respectively

*Superscript*

0 = value at the component midplane

Received Aug. 7, 1991; revision received Nov. 13, 1991; accepted for publication Nov. 22, 1991. 
*Research Associate, Department of Aerospace Engineering.
†Professor, Department of Aerospace Engineering. Member AIAA.

## Introduction

As the demand for high performance structures is increased, sandwich plates receive new attention. Sandwich plates have been widely used because of high-specific bending stiffness. When they are used in the form of full-depth honeycomb sandwich plates, such as wings or control surfaces, the sandwich plate is of nonconstant thickness. Tapered anisotropic sandwich plates are very interesting structures because of several design variables such as stacking sequences of faces, face-to-core thickness ratio, combination of material properties, and taper ratio.

For the analysis of uniform thickness cases, numerous approximating solutions were given by many authors such as Kim and Hong[1] and Monforton and Ibrahim.[2] They considered material anisotropy, face bending stiffness,[1,2] and finite bonding stiffness.[1] A closed-form solution for sandwich beam was given by Ojalvo.[3] On the other hand, as in finite element analysis, tapered sandwich plates have received far less attention in analytic work than have plates of uniform thickness.

The tapered sandwich beam was analyzed by Huang and Alspaugh[4] by the sandwich plate theory using the constitutive equations of locally constant thickness. Akasaka and Asano[5] analyzed simply supported sandwich panels with sinusoidally varying thickness. They showed the importance of shell effect on the curvature by the flattening effect of faces. Paydar and others employed the finite difference method to calculate the

deflections and core shear stresses for tapered square[6,7] and annular sandwich plate.[8] The bending problem for a cantilevered sandwich beam with thickness variation was analyzed by Libove and Lu.[9] The finite element analysis was performed by Holt and Webber[10] for arbitrary thickness variation of sandwich structures.

Recently, Jeon and Hong[11] used the Rayleigh-Ritz method for an approximate solution of tapered sandwich structures with anisotropic composite faces. They clearly showed the difference between the uniform and tapered sandwich plate in the explicit expressions. By some numerical examples of tapered sandwich beams, they concluded that the structural curvature changes its sign locally and the conventional antisymmetric deformation assumption for faces must be reexamined.

In the present work, tapered sandwich plates with arbitrary edge conditions are analyzed. The face coupling and bending stiffness in addition to the inplane stiffness are included. Three local coordinate systems are introduced for each component. The analysis takes into account the geometric coupling between the core shear strain and the face normal deflection existing only for the tapered geometry. Some numerical examples are presented for sandwich plates to confirm the versatility of the method.

## Governing Equations

### Total Potential Energy

The assumptions made for the analysis are as follows: The tapered sandwich plate is geometrically symmetric about its midplane. The thicknesses of anisotropic faces are constant and *moderately* thick to apply the classical lamination theory (CLT). The core is orthotropic and the core thickness decreases linearly in one direction. The core is inextensible in the thickness direction and can only be deformable in transverse shear. The faces and the core are perfectly bonded altogether in the interfaces. Each component is under the small deformation. An overall view of the tapered sandwich plate under consideration is shown in Fig. 1.

The thickness of the core decreases linearly in the $x$ direction as

$$h(x) = h_0 - x\tan\beta \tag{1}$$

When the core is rotated about its reference axes by $\phi_c$, the strain energy in the core can be written as:

$$U_c = \frac{1}{2}\iiint \begin{Bmatrix}\gamma^0_{yz}\\ \gamma^0_{xz}\end{Bmatrix}_c^T \begin{bmatrix}\overline{Q}_{44} & \overline{Q}_{45}\\ \overline{Q}_{45} & \overline{Q}_{55}\end{bmatrix}_c \begin{Bmatrix}\gamma^0_{yz}\\ \gamma^0_{xz}\end{Bmatrix}_c dV_c \tag{2}$$

where

$$\overline{Q}_{44} = G_{23}\cos^2\phi_c + G_{13}\sin^2\phi_c$$

$$\overline{Q}_{45} = (G_{13} - G_{23})\cos\phi_c\sin\phi_c$$

$$\overline{Q}_{55} = G_{13}\cos^2\phi_c + G_{23}\sin^2\phi_c$$

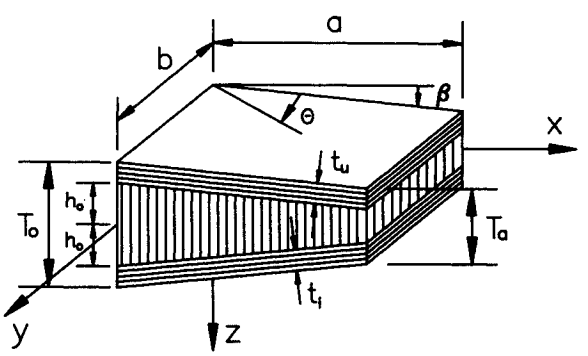


**Fig. 1 Geometry of tapered sandwich plate with anisotropic laminated faces.**

The superscript 0 in Eq. (2) means the values at the core midplane, subscript $c$ for the core and $G_{13}$, $G_{23}$ are the core transverse shear moduli about its material principal axes. Substituting Eq. (1) into Eq. (2) and integrating over the core thickness give

$$U_c = \frac{1}{2}\iint \begin{Bmatrix}\gamma^0_{yz}\\ \gamma^0_{xz}\end{Bmatrix}_c^T \{[G^0_{ij}] - x[H^0_{ij}]\} \begin{Bmatrix}\gamma^0_{yz}\\ \gamma^0_{xz}\end{Bmatrix}_c dxdy \tag{3}$$

where

$$[G^0_{ij}] = 2h_0\,[\overline{Q}_{ij}]_c$$

$$[H^0_{ij}] = 2\tan\beta\,[\overline{Q}_{ij}]_c, \quad i, j = 4, 5$$

The present sandwich plate is tapered by the thickness variation of core and face slope about the midplane of the structure. To employ the Rayleigh-Ritz method for an approximate solution, three local coordinate systems for each component are introduced, as shown in Fig. 2.

The normal displacements of the upper and lower faces are the same by the previous assumptions and only the directions of the unit vectors are different due to the face slope. Therefore, the expression for the normal displacement of each face can be written as one variable and the six variables for two faces are reduced to five.

$$u_{su}(s, y, n) = u^0_{su}(s, y) - n_u\frac{\partial u^0_n}{\partial s} \tag{4a}$$

$$u_{yu}(s, y, n) = u^0_{yu}(s, y) - n_u\frac{\partial u^0_n}{\partial y} \tag{4b}$$

$$u_n(s, y, n) = u^0_n(s, y) \tag{4c}$$

$$u_{sl}(s, y, n) = u^0_{sl}(s, y) - n_l\frac{\partial u^0_n}{\partial s} \tag{4d}$$

$$u_{yl}(s, y, n) = u^0_{yl}(s, y) - n_l\frac{\partial u^0_n}{\partial y} \tag{4e}$$

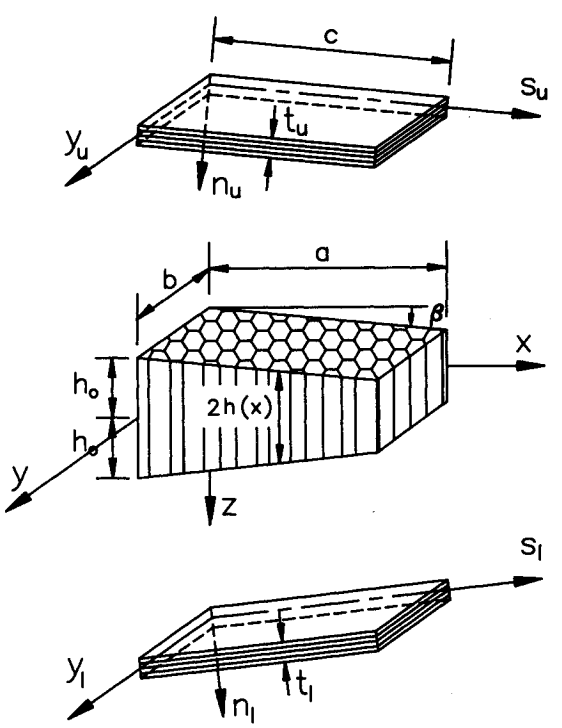


**Fig. 2 Local coordinate systems for each component.**

where superscript 0 means the values at the face midplane. Based upon the CLT, the strain energy of upper face can be written as:

$$U_{fu} = \frac{1}{2}\iiint \{\sigma_{ss}\varepsilon_{ss} + \sigma_{yy}\varepsilon_{yy} + \tau_{sy}\gamma_{sy}\}_u \, dV_{fu} \quad (5)$$

Substituting the constitutive equations and integrating the above Eq. (5) over the face thickness give

$$U_{fu} = \frac{1}{2}\iint \{\varepsilon^0\}_u^T[A_{ij}]_u\{\varepsilon^0\}_u \, dsdy + \iint \{\varepsilon^0\}_u^T[B_{ij}]_u\{\kappa\} \, dsdy + \frac{1}{2}\iint \{\kappa\}^T[D_{ij}]_u\{\kappa\} \, dsdy \quad (6)$$

where $[A_{ij}]_u$, $[B_{ij}]_u$, and $[D_{ij}]_u$ are the extensional, coupling, and bending stiffness matrices of upper face, respectively, as defined in Ref. 12. Similarly, the expression for the lower face can be written as:

$$U_{fl} = \frac{1}{2}\iint \{\varepsilon^0\}_l^T[A_{ij}]_l\{\varepsilon^0\}_l \, dsdy + \iint \{\varepsilon^0\}_l^T[B_{ij}]_l\{\kappa\} \, dsdy + \frac{1}{2}\iint \{\kappa\}^T[D_{ij}]_l\{\kappa\} \, dsdy \quad (7)$$

Under the normal distributed load $q_1$, vertical distributed load, $q_2$, and vertical concentrated load, $Q_0$, in the upper face, potential energy by external works can be expressed as:

$$V = -\iint q_1(s, y)\, u_n^0(s, y) \, dsdy - \iint q_2(x, y)\, w^0(x, y) \, dxdy - Q_0(x_0, y_0)\, w^0(x_0, y_0) \quad (8)$$

**Compatibility Conditions**

Using three local coordinate systems for the upper face, lower face, and the core, compatibility conditions give the explicit expressions for the core transverse shear strains in terms of upper and lower face displacements as:

$$\gamma_{xz}^0 = \frac{\partial w^0}{\partial x} - \frac{1}{2h(x)}[(u_{su} - u_{sl})\cos\beta - 2u_n^0 \sin\beta] \quad (9a)$$

$$\gamma_{yz}^0 = \frac{\partial w^0}{\partial y} - \frac{1}{2h(x)}[u_{yu} - u_{yl}] \quad (9b)$$

$$w^0 = \frac{1}{2}(u_{su} - u_{sl})\sin\beta + u_n^0 \cos\beta \quad (9c)$$

where $u_{su}$, $u_{yu}$, $u_{sl}$, and $u_{yl}$ are the face displacements at the interfaces. The difference from the uniform thickness case (see Ref. 13) is expressed in Eqs. (9a) and (9c). The transverse shear strain $\gamma_{xz}^0$ in core and the structural deflection $w^0$ are determined both from the face inplane displacements and from the face normal deflection for the nonzero of $\beta$.

**Displacements Assumptions**

To apply arbitrary edge conditions, all the displacements can be expressed in general form, as in Ref. 14. The displacements of each face are expressed by unknown coefficients $C_{mn}^1 - C_{mn}^5$ and the proper shape functions $\phi_{mn}^1 - \phi_{mn}^3$ satisfying the given edge conditions as:

$$u_{su}^0(s, y) = \sum_m \sum_n C_{mn}^1 \phi_{mn}^1(s, y) = \{\phi_{mn}^1\}^T\{C_{mn}^1\} \quad (10a)$$

$$u_{yu}^0(s, y) = \sum_m \sum_n C_{mn}^2 \phi_{mn}^2(s, y) = \{\phi_{mn}^2\}^T\{C_{mn}^2\} \quad (10b)$$

$$u_n^0(s, y) = \sum_m \sum_n C_{mn}^3 \phi_{mn}^3(s, y) = \{\phi_{mn}^3\}^T\{C_{mn}^3\} \quad (10c)$$

$$u_{sl}^0(s, y) = \sum_m \sum_n C_{mn}^4 \phi_{mn}^1(s, y) = \{\phi_{mn}^1\}^T\{C_{mn}^4\} \quad (10d)$$

$$u_{yl}^0(s, y) = \sum_m \sum_n C_{mn}^5 \phi_{mn}^2(s, y) = \{\phi_{mn}^2\}^T\{C_{mn}^5\} \quad (10e)$$

Substituting the above expressions to the strain energy and the potential energy by external works gives

$$U_c = \frac{1}{2}\cos\beta\{C\}^T([K^1] - [K^2])\{C\} \quad (11a)$$

$$U_{fu} = \frac{1}{2}\begin{Bmatrix} C_{mn}^1 \\ C_{mn}^2 \end{Bmatrix}^T [K^3] \begin{Bmatrix} C_{mn}^1 \\ C_{mn}^2 \end{Bmatrix} + \begin{Bmatrix} C_{mn}^1 \\ C_{mn}^2 \end{Bmatrix}^T [K^4]\{C_{mn}^3\} + \frac{1}{2}\{C_{mn}^3\}^T[K^5]\{C_{mn}^3\} \quad (11b)$$

$$U_{fl} = \frac{1}{2}\begin{Bmatrix} C_{mn}^4 \\ C_{mn}^5 \end{Bmatrix}^T [K^6] \begin{Bmatrix} C_{mn}^4 \\ C_{mn}^5 \end{Bmatrix} + \begin{Bmatrix} C_{mn}^4 \\ C_{mn}^5 \end{Bmatrix}^T [K^7]\{C_{mn}^3\} + \frac{1}{2}\{C_{mn}^3\}^T[K^8]\{C_{mn}^3\} \quad (11c)$$

$$V = -\{C\}^T\{F\} \quad (11d)$$

where

$$\{C\}^T = [\{C_{mn}^1\}^T, \{C_{mn}^2\}^T, \{C_{mn}^3\}^T, \{C_{mn}^4\}^T, \{C_{mn}^5\}^T]$$

$$\{F\}^T = [\{F_{mn}^1\}^T, \{0\}^T, \{F_{mn}^3\}^T, \{0\}^T, \{0\}^T]$$

Detailed expressions from $[K^1]$ to $[K^8]$ and related quantities are given in the Appendix and the components of equivalent force vector $\{F\}$ are given below.

$$\{F_{mn}^1\} = Q_0(x_0, y_0)\sin\beta\cos\beta\{\phi_{mn}^1\}_{(x0,y0)} + \sin\beta\cos\beta\iint q_2(s, y)\{\phi_{mn}^1\} \, dsdy \quad (12a)$$

$$\{F_{mn}^3\} = \iint q_1(s, y)\{\phi_{mn}^3\} \, dsdy + \frac{t_u}{2}\sin\beta\cos\beta \times \left\{Q_0(x_0, y_0)\{\phi_{mn}^8\}_{(x0,y0)} + \iint q_2(s, y)\{\phi_{mn}^8\} \, dsdy\right\} + \cos^2\beta\left\{Q_0(x_0, y_0)\{\phi_{mn}^3\}_{(x0,y0)} + \iint q_2(s, y)\{\phi_{mn}^3\} \, dsdy\right\} \quad (12b)$$

**Approximate Solution**

To get an approximate solution, the principle of minimum total potential energy is applied. The partial differentiation of the total potential energy with respect to each unknown coefficient is expressed as:

$$\frac{\partial \Pi}{\partial C_{mn}^i} = 0, \quad i = 1, \ldots, 5 \quad (13)$$

Rearranging the above gives a linear matrix equation as:

$$[g_{ij}]\{C^j\} = \{F_i\}, \quad i, j = 1, \ldots, 5 \tag{14}$$

where $[g_{ij}]$ is the symmetric equivalent stiffness matrix having $5 \times 5$ submatrices. Detailed expressions for each submatrix can be obtained directly from the partial differentiation of the total potential energy. By solving this matrix equation, the unknown coefficients are obtained and all the related quantities can be determined.

## Results and Discussion

### Verification of the Analysis

The uniform sandwich plates under all simply supported edge conditions are analyzed for comparisons at first. The shape functions used are given below.

$$\phi^1_{mn} = \cos\frac{m\pi s}{c}\sin\frac{n\pi y}{b} \tag{15a}$$

$$\phi^2_{mn} = \sin\frac{m\pi s}{c}\cos\frac{n\pi y}{b} \tag{15b}$$

$$\phi^3_{mn} = \sin\frac{m\pi s}{c}\sin\frac{n\pi y}{b} \tag{15c}$$

The material properties are $E_1 = 206.43$ GPa ($30 \times 10^6$ psi), $E_1/E_2 = 40$, $G_{12}/E_2 = 1.0$, $\nu_{12} = 0.25$, $G_{13} = 116.98$ MPa (17,000 psi) and $G_{23} = 240.84$ MPa (35,000 psi). The dimensions are $a = 1.27$ m (50 in.), $2h_0 = 0.0254$ m (1 in.) and $q_1 = 6881.1$ N/m$^2$ (1 lb/in.$^2$). The remaining dimensions are determined from the geometric parameters. The stacking sequence of the sandwich plate is $[90/0/\text{core}/90/0]_T$. The core rotation angle $\phi_c$ is zero. Five effective expansion terms in both directions are taken in the displacement assumptions for the calculations. The IMSL subroutine DMLIN was used for numerical integration. The midpoint deflections and the resultant forces in both faces are compared with those of previous results of Ref. 2 in Table 1. They show very good agreement.

The comparisons based upon the structural deflections are performed for the tapered sandwich beams with the results of previous experiments and finite difference method in Ref. 6. Experimental geometry, loading and boundary conditions are shown in upper side in Fig. 3. Because the thickness of core in the present analysis decreases linearly in $x$ direction, the experiment is modeled as shown in the lower side of Fig. 3. The shape functions used are given below:

$$\phi^1_{mn} = \sin\frac{m\pi s}{2c} \tag{16a}$$

$$\phi^2_{mn} = 0 \tag{16b}$$

$$\phi^3_{mn} = 1 - \cos\frac{m\pi s}{2c} \tag{16c}$$

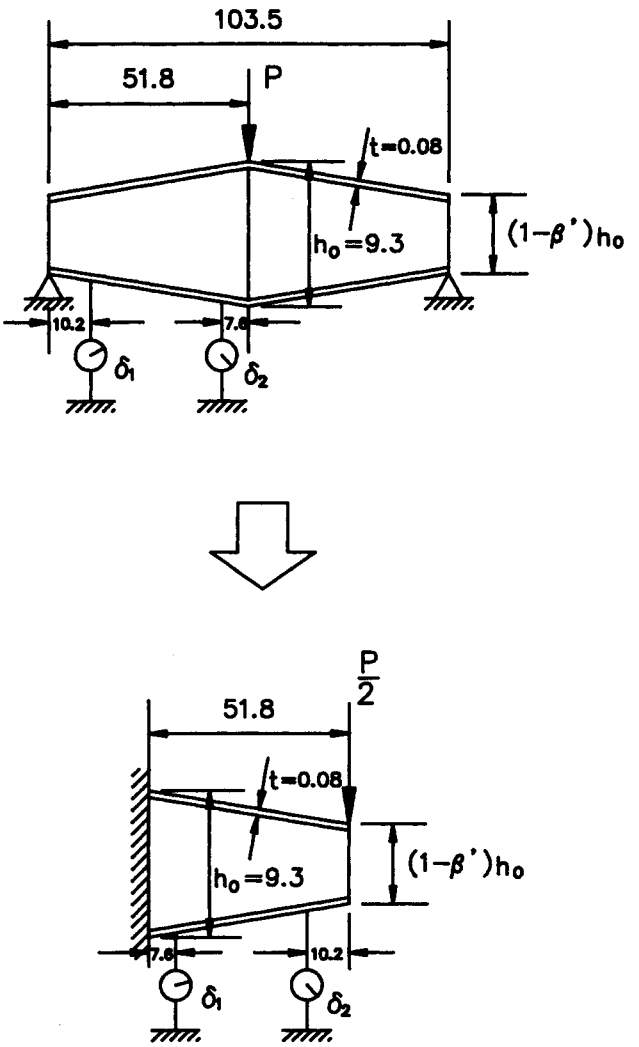


**Fig. 3 Modeling of previous experiment for comparison of "quasi-stiffness."**

**Table 2 Comparisons of *quasistiffness* between the present results and the previously reported experimental and theoretical results**

| | $P/(\delta_2 - \delta_1)$, KPa | | |
|---|---|---|---|
| *HR* | FDM[6] | Exp.[6] | Present |
| 1.00 | 1772 | 1772 | 1773.8 |
| 1.11 | 1848 | 1779 | 1851.3 |
| 1.43 | 2034 | 1986 | 2047.5 |
| 2.00 | 2289 | 2282 | 2332.5 |

**Table 1 Deflections and resultant forces at $x = a/2$ and $y = b/2$ for uniform sandwich plate of $[90/0/\text{core}/90/0]_T$ with all simply supported edge conditions ($a = 1.27$ m, $q_0 = 6881.1$ N/m$^2$, $2h_0 = 0.0254$ m)**

| *AR*, *a*/*b* | $2h_0/t_l$ | $w^{0\,2}$, m | $w^0$(present), m | $N_x^2$, N/m | $N_x$(present), N/m |
|---|---|---|---|---|---|
| 1.0 | 4 | $5.121 \times 10^{-4}$ | $5.123 \times 10^{-4}$ | +21780[a]<br>−21780[b] | +21920[a]<br>−21798[b] |
| | 10 | $1.421 \times 10^{-3}$ | $1.422 \times 10^{-3}$ | +26360[a]<br>−26360[b] | +26587[a]<br>−26395[b] |
| 2.5 | 4 | $4.168 \times 10^{-5}$ | $4.188 \times 10^{-5}$ | +1268.7[a]<br>−1274.8[b] | +1318.5[a]<br>−1293.3[b] |
| | 10 | $9.103 \times 10^{-5}$ | $9.141 \times 10^{-5}$ | +1061.7[a]<br>−1064.2[b] | +1122.4[a]<br>−1095.5[b] |

[a]For lower face.
[b]For upper face.

The material used for faces are Al alloy of $E = 68.17$ GPa, $\nu = 0.3$ and for core are polystyrene of $G_{13} = G_{23} = 3.68$ MPa. Fifteen effective terms in the displacement assumptions are taken in $x$-direction. From the deflections at two points, the *quasistiffness* is calculated. The comparisons are shown in Table 2. The present calculations show more stiff results about 0.1–4.0% than those of the previous experiments. Considering factors such as the difference in modeling itself and experimental errors, the present analysis can be said to give good results.

The structural midplane deflections are compared with those of the finite difference method in Ref. 6 for the tapered sandwich plates. The boundary condition is free (F) at the thin edge ($x = a$) and simply supported (S) at three edges (abbreviated to SSFS, counterclockwise from the edge at $x = 0$). The shape functions used are given below

$$\phi^1_{mn} = \cos\frac{m\pi s}{2c}\sin\frac{n\pi y}{b} \tag{17a}$$

$$\phi^2_{mn} = \sin\frac{m\pi s}{2c}\cos\frac{n\pi y}{b} \tag{17b}$$

$$\phi^3_{mn} = \sin\frac{m\pi s}{2c}\sin\frac{n\pi y}{b} \tag{17c}$$

The external load is sinusoidal as $q_2(x, y) = q_2 \sin(\pi x/a) \sin(\pi y/b)$. The material is isotropic of $E = 251$ GPa, $\nu_{12} = 0.3$ and isotropic core. The dimensions are $a = b = 0.5$ m, $t_u = t_l = 0.005$ m and $T_0 = 0.025$ m. After the convergence tests, eight and three effective terms in the displacement assumptions are taken in $x$ and $y$ directions, respectively.

The deflections are shown in Fig. 4 for various core shear moduli along $y = b/2$ ($HR = 2.0$). The deflections by the present analysis are smaller than those of previous work in the literature because the faces in Ref. 6 are treated as membranes by neglecting the face-bending stiffness for the *thick* faces. But the present analysis includes the face-bending stiffness as well (by CLT) and, therefore, shows more stiff results. As the core shear rigidity $R_x$ decreases, the differences are getting smaller.

**Illustrative Examples**

The material properties used for faces are $E_1 = 181.0$ GPa, $E_2 = 10.7$ GPa, $G_{12} = 7.07$ GPa, and $\nu_{12} = 0.28$. Those for core are $G^*_{13} = 110.32$ MPa and $G^*_{23} = 44.128$ MPa (see Ref. 15). The dimensions taken are $a = 1$ m, $t_u = t_l = 0.001$ m and $T_0 = 0.025$ m. The remaining dimensions are determined from the geometric parameters.

For the first case, SSFS edge conditions are used. The used shape functions are same as in Eq. (17). The structure is under the uniform normal distributed load as $q_1(s, y) =$ constant. The stacking sequence of the sandwich plate is $[90/0/\text{core}/90/0]_T$. The core rotation angle $\phi_c$ hereafter is set to zero.

As the taper ratio $HR$ is increased from 1.0 to 10.0, the deflections at the $x = a$ and $y = b/2$ are shown in Fig. 5 for various core moduli ratios ($AR = 2.0$). As the taper ratio increases, the deflection increases up to a certain taper ratio and then decreases. This is due to the change of the dominant factor for the structural stiffness from the stiffness reduction by the core volume change to the increase of the face slope participation. The deflections along $y = b/2$ are shown in Fig. 6 ($HR = 1.0$, $AR = 2.0$) and Fig. 7 ($HR = 2.0$, $AR =$

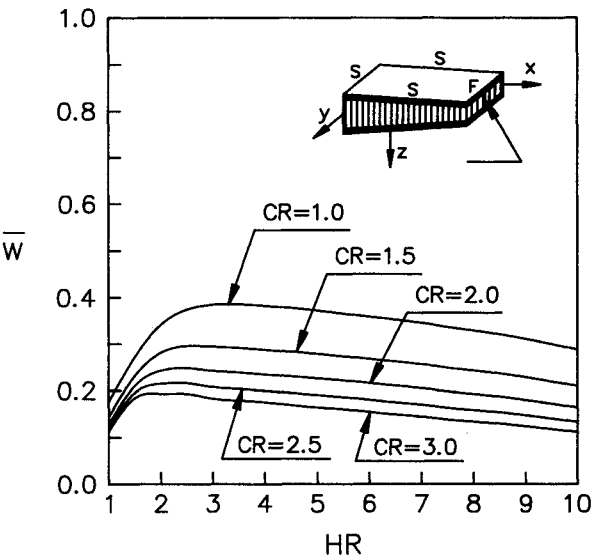


**Fig. 5 Effect of taper ratio $HR$ on the deflection at $x = a$ and $y = b/2$ for various core shear moduli under SSFS edge conditions with $[90/0/\text{core}/90/0]_T$ ($AR = 2.0$).**

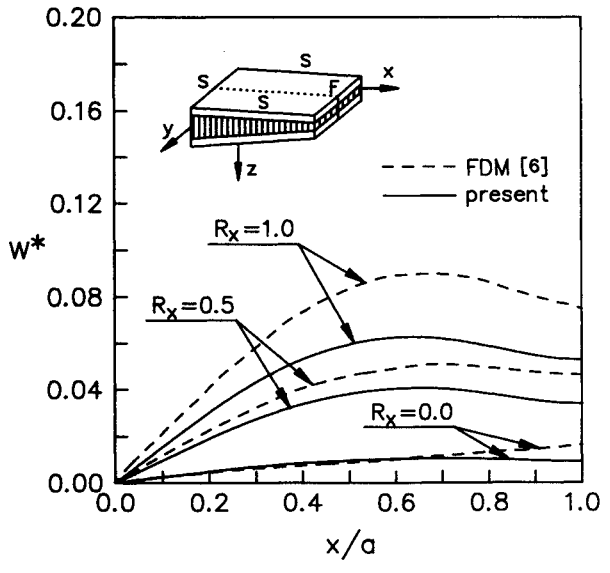


**Fig. 4 Comparisons of deflections along $y = b/2$ for various core shear moduli with SSFS edge conditions.**

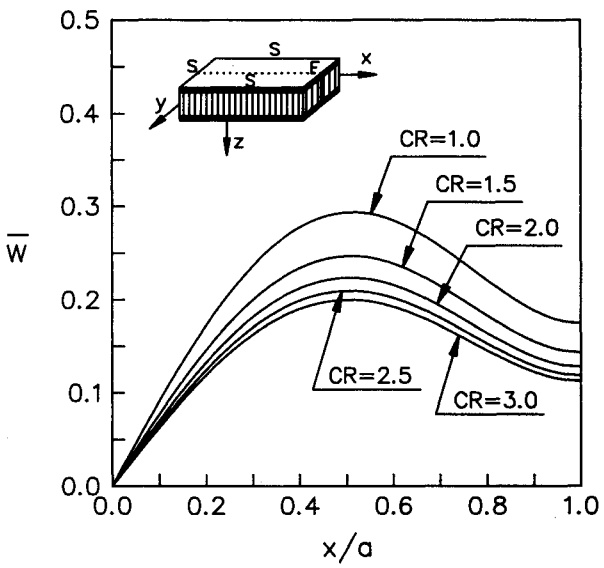


**Fig. 6 The deflections along $y = b/2$ for various core shear moduli ratio $CR$ under SSFS edge conditions with $[90/0/\text{core}/90/0]_T$ ($HR = 1.0$, $AR = 2.0$).**

2.0) for various core moduli ratios. The deflections are more influenced by core shear moduli for the tapered case than those for the uniform case.

The effect of face-stacking sequence is examined for the *SSFS* edge conditions. The stacking sequences taken for comparisons are three cases of $[0/90/\text{core}/90/0]_T$, $[90/0/\text{core}/90/0]_T$ and $[90/0/\text{core}/0/90]_T$. The deflections along $y = b/2$ are shown in Fig. 8 ($HR = 1.0$, $AR = 2.0$) and Fig. 9 ($HR = 2.0$, $AR = 2.0$). They show a little difference in their magnitudes.

For the second case, the edge conditions of clamped ($C$) at $x = 0$, free ($F$) at $x = a$, and simply supported ($S$) at $y = 0$, $b$ (abbreviated to *CSFS*) are used. The shape functions used are given below.

$$\phi^1_{mn} = \sin\frac{m\pi s}{2c}\sin\frac{n\pi y}{b} \tag{19a}$$

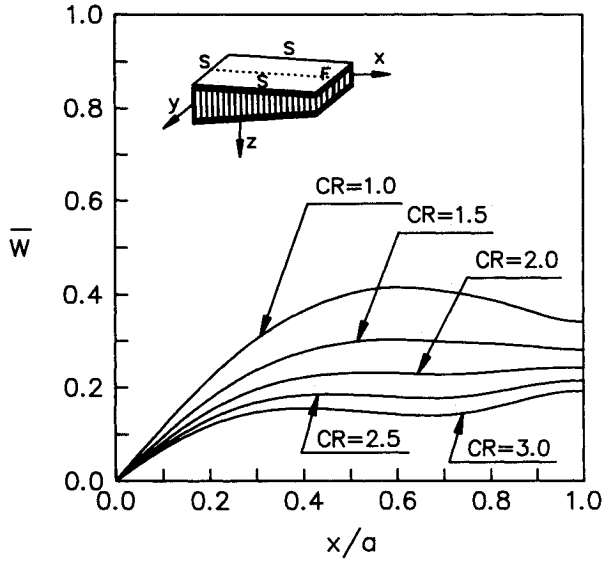


**Fig. 7 The deflections along $y = b/2$ for various core shear moduli ratio $CR$ under SSFS edge conditions with $[90/0/\text{core}/90/0]_T$ ($HR = 2.0$, $AR = 2.0$).**

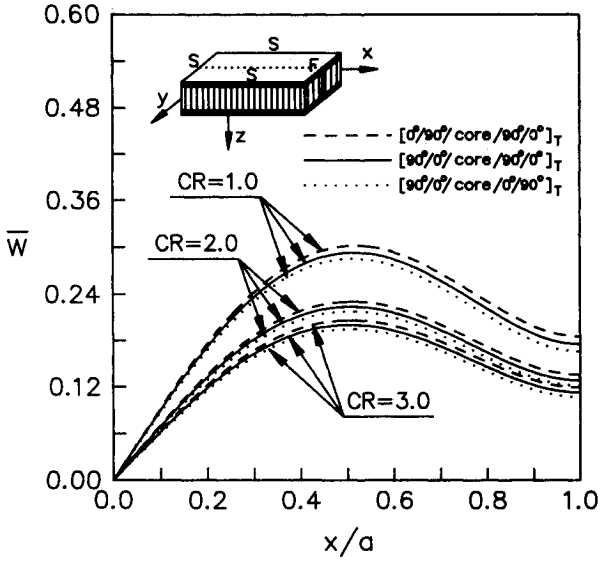


**Fig. 8 Effect of stacking sequence on the deflection along $y = b/2$ with SSFS edge conditions ($HR = 1.0$, $AR = 2.0$).**

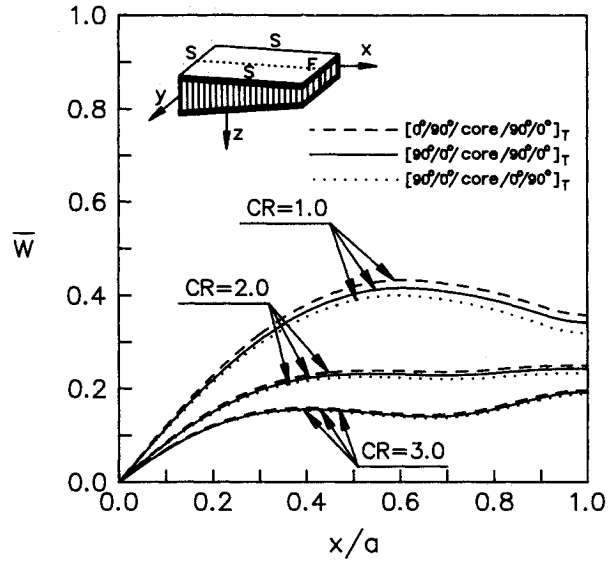


**Fig. 9 Effect of stacking sequence on the deflection along $y = b/2$ with SSFS edge conditions ($HR = 2.0$, $AR = 2.0$).**

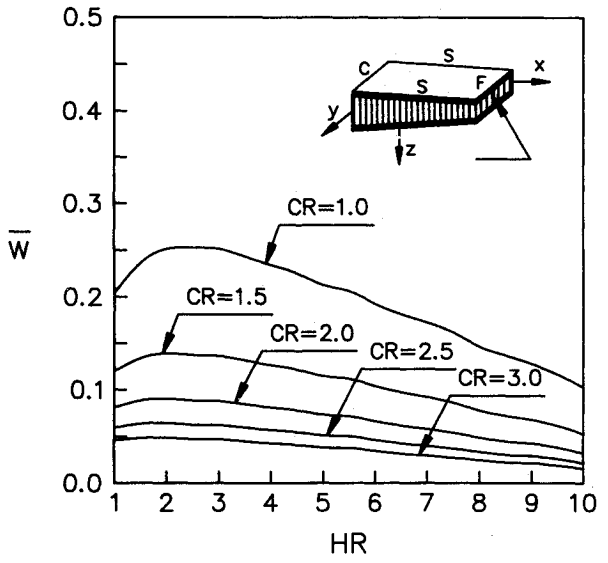


**Fig. 10 Effect of taper ratio $HR$ on the deflection at $x = a$ and $y = b/2$ for various core shear moduli under CSFS edge conditions with $[90/0/\text{core}/90/0]_T$ ($AR = 2.0$).**

$$\phi^2_{mn} = \sin\frac{m\pi s}{2c}\cos\frac{n\pi y}{b} \tag{19b}$$

$$\phi^3_{mn} = \left(1 - \cos\frac{m\pi s}{2c}\right)\sin\frac{n\pi y}{b} \tag{19c}$$

As the taper ratio $HR$ is increased from 1.0 to 10.0, the deflections at the $x = a$ and $y = b/2$ are shown in Fig. 10 for various core moduli ratios ($AR = 2.0$). The trend of deflection increase or decrease is influenced more by the core shear moduli ratios for the high taper ratios than that for the *SSFS* edge conditions. The deflections along $y = b/2$ are shown in Fig. 11 ($HR = 1.0$, $AR = 2.0$) and Fig. 12 ($HR = 2.0$, $AR = 2.0$) for various core moduli ratios. The deflections are less influenced by core shear moduli for the taper ratios between 1.0 and 2.0.

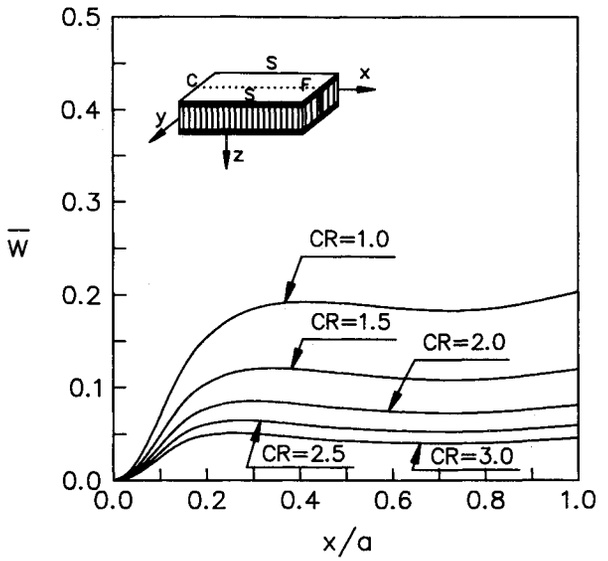


**Fig. 11 The deflection along $y = b/2$ for various core shear moduli ratio $CR$ under CSFS edge conditions with $[90/0/\text{core}/90/0]_T$ ($HR = 1.0$, $AR = 2.0$).**

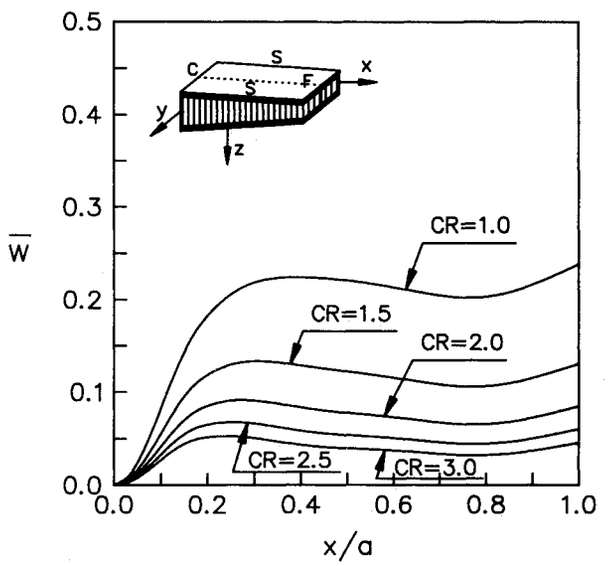


**Fig. 12 The deflection along $y = b/2$ for various core shear moduli ratio $CR$ under CSFS edge conditions with $[90/0/\text{core}/90/0]_T$ ($HR = 2.0$, $AR = 2.0$).**

## Conclusions

A new approximate method is used for the analysis of the tapered sandwich plates with anisotropic laminated faces and an orthotropic core. Local coordinate systems for each component are introduced. The faces are analyzed by the classical lamination theory. The inplane displacements of each face are taken as independent variables. For the tapered case, it is shown that the core shear strain is related directly to the face normal deflection. The total potential energy is obtained and the Rayleigh-Ritz method is employed for an approximate solution. The present formulation can be applied to arbitrary edge conditions.

The comparisons based upon the deflections with those of previous works confirmed the validity of the present method. The numerical calculations for various edge conditions, taper ratios, core moduli ratios, and stacking sequence are performed. As the taper ratio increases, the deflection increases up to certain taper ratio and then decreases by the contribution ratio change of each component to the structural stiffness. The increasing or decreasing trend is dependent upon the material properties, taper ratios, and the edge conditions. The deflection is more affected by the core shear modulus for the tapered case than for the uniform case.

## Appendix

The matrices from $[K^1]$ to $[K^8]$ defined in Eq. (11) and related quantities are shown below:

$$[K^1] = \iint [R]\,[G_{ij}^0]\,[R]^T\,dsdy \tag{A1}$$

$$[K^2] = \iint s\cos\beta\,[R]\,[H_{ij}^0]\,[R]^T\,dsdy \tag{A2}$$

$$[K^3] = \iint [P^1]\,[A_{ij}]_u[P^1]^T\,dsdy \tag{A3}$$

$$[K^4] = \iint [P^1]\,[B_{ij}]_u[P^2]^T\,dsdy \tag{A4}$$

$$[K^5] = \iint [P^2]\,[D_{ij}]_u[P^2]^T\,dsdy \tag{A5}$$

$$[K^6] = \iint [P^1]\,[A_{ij}]_l[P^1]^T\,dsdy \tag{A6}$$

$$[K^7] = \iint [P^1]\,[B_{ij}]_l[P^2]^T\,dsdy \tag{A7}$$

$$[K^8] = \iint [P^2]\,[D_{ij}]_l[P^2]^T\,dsdy \tag{A8}$$

$$[R] = \begin{bmatrix} R_1^y & R_1^x \\ R_2^y & 0 \\ R_3^y & R_3^x \\ R_4^y & R_4^x \\ R_5^y & 0 \end{bmatrix} \tag{A9}$$

$$R_1^y = \tfrac{1}{2}\sin\beta\,\{\phi_{mn}^5\} \tag{A10}$$

$$R_2^y = -\frac{1}{2h(x)}\{\phi_{mn}^2\} \tag{A11}$$

$$R_3^y = \frac{(t_u + t_l)}{4}\sin\beta\,\{\phi_{mn}^{11}\} + \frac{(t_u + t_l)}{4h(x)}\{\phi_{mn}^9\} + \cos\beta\,\{\phi_{mn}^9\} \tag{A12}$$

$$R_4^y = -\tfrac{1}{2}\sin\beta\,\{\phi_{mn}^5\} \tag{A13}$$

$$R_5^y = \frac{1}{2h(x)}\{\phi_{mn}^2\} \tag{A14}$$

$$R_1^x = \frac{1}{2}\tan\beta\,\{\phi_{mn}^4\} - \frac{\cos\beta}{2h(x)}\{\phi_{mn}^1\} \tag{A15}$$

$$R_3^x = \frac{(t_u + t_l)}{4}\tan\beta\,\{\phi_{mn}^{10}\} + \frac{(t_u + t_l)}{4h(x)}\cos\beta\,\{\phi_{mn}^8\} + \frac{\sin\beta}{h(x)}\{\phi_{mn}^3\} + \{\phi_{mn}^8\} \tag{A16}$$

$$R_4^x = -\frac{1}{2}\tan\beta\,\{\phi_{mn}^4\} + \frac{1}{2h(x)}\cos\beta\,\{\phi_{mn}^1\} \tag{A17}$$

$$[P^1] = \begin{bmatrix} \{\phi_{mn}^4\} & \{0\} & \{\phi_{mn}^5\} \\ \{0\} & \{\phi_{mn}^7\} & \{\phi_{mn}^6\} \end{bmatrix} \tag{A18}$$

$$[P^2] = [\{\phi_{mn}^{10}\}\,\{\phi_{mn}^{11}\}\,\{\phi_{mn}^{12}\}] \tag{A19}$$

$$\phi_{mn}^4 = \frac{\partial\phi_{mn}^1}{\partial s} \tag{A20}$$

$$\phi_{mn}^5 = \frac{\partial\phi_{mn}^1}{\partial y} \tag{A21}$$

$$\phi_{mn}^6 = \frac{\partial\phi_{mn}^2}{\partial s} \tag{A22}$$

$$\phi^7_{mn} = \frac{\partial \phi^2_{mn}}{\partial y} \tag{A23}$$

$$\phi^8_{mn} = \frac{\partial \phi^3_{mn}}{\partial s} \tag{A24}$$

$$\phi^9_{mn} = \frac{\partial \phi^3_{mn}}{\partial y} \tag{A25}$$

$$\phi^{10}_{mn} = -\frac{\partial^2 \phi^3_{mn}}{\partial s^2} \tag{A26}$$

$$\phi^{11}_{mn} = -\frac{\partial^2 \phi^3_{mn}}{\partial y^2} \tag{A27}$$

$$\phi^{12}_{mn} = -2\frac{\partial^2 \phi^3_{mn}}{\partial s \partial y} \tag{A28}$$

## References


[1]Kim, C. G., and Hong, C. S., "Buckling of Unbalanced Anisotropic Sandwich Plates with Finite Bonding Stiffness," *AIAA Journal*, Vol. 26, No. 8, 1988, pp. 982–988.

[2]Monforton, G. R., and Ibrahim, I. M., "Analysis of Sandwich Plates with Unbalanced Cross-Ply Faces," *International Journal of Mechanical Sciences*, Vol. 17, No. 3, 1975, pp. 227–238.

[3]Ojalvo, I. U., "Departures from Classical Beam Theory in Laminated Sandwich and Short Beams," *AIAA Journal*, Vol. 15, No. 10, 1977, pp. 1518–1521.

[4]Huang, S. N., and Alspaugh, D. W., "Minimum Weight Sandwich Beam Design," *AIAA Journal*, Vol. 12, No. 12, 1974, pp. 1617–1618.

[5]Akasaka, T., and Asano, K., "Stress and Deformation of the Sandwich Panel Having Curved Faceplates Under Pressure Loading," *Recent Advances in Composites in the United States and Japan*, American Society for Testing and Materials/STP 864, 1985, pp. 263–277.

[6]Paydar, N., and Libove, C., "Stress Analysis of Sandwich Plates with Unidirectional Thickness Variation," *Journal of Applied Mechanics*, Vol. 53, No. 3, 1986, pp. 609–613.

[7]Paydar, N., and Libove, C., "Bending of Sandwich Plates of Variable Thickness," *Journal of Applied Mechanics*, Vol. 55, No. 2, 1988, pp. 419–424.

[8]Paydar, N., "Stress Analysis of Annular Sandwich Plates of Linearly Varying Thickness," *International Journal of Solids and Structures*, Vol. 24, No. 3, 1988, pp. 313–320.

[9]Libove, C., and Lu, C. H., "Beam-like Bending of Variable-Thickness Sandwich Plates," *AIAA Journal*, Vol. 27, No. 4, 1989, pp. 500–507.

[10]Holt, P. J., and Webber, J. P. H., "Finite Elements for Honeycomb Sandwich Plates and Shells, Part 2: Numerical Results and Testing," *Aeronautical Journal*, Vol. 84, No. 832, 1980, pp. 157–167.

[11]Jeon, J. S., and Hong, C. S., "Analysis of Tapered Sandwich Structures with Anisotropic Composite Faces," to appear in the *Computers & Structures* (May 1991).

[12]Jones, R. M., *Mechanics of Composite Materials*, McGraw-Hill, New York, 1975, pp. 147–156.

[13]Allen, H. G., *Analysis and Design of Structural Sandwich Panels*, Pergamon, Oxford, England, UK, 1969, pp. 200–207.

[14]Baharlou, B., and Leissa, A. W., "Vibration and Buckling of Generally Laminated Composite Plates with Arbitrary Edge Conditions," *International Journal of Mechanical Sciences*, Vol. 29, No. 8, 1987, pp. 545–555.

[15]Lubin, G. (ed.), *Handbook of Composites*, Van Nostrand Reinhold, New York, 1984, pp. 557–601.